J Polym Environ
DOI 10.1007/s10924-010-0240-x

ORIGINAL PAPER

Mechanical and Thermal Properties of PLLA/PCL Modified Clay Nanocomposites

Wisam H. Hoidy · Emad A. Jaffar Al-Mulla · Khalid W. Al-Janabi

Abstract Poly(L-lactic acid) (PLLA)/poly(caprolactone) (PCL) and two types of organoclay (OMMT) including a fatty amide and ocatdecylamine montmorillonite (FA-MMT and ODA-MMT) were employed to produce polymer nanocomposites by melt blending. Materials were characterized using X-ray diffraction (XRD), Fourier transform infrared (FTIR) spectroscopy, thermogravimetric analysis (TGA), elemental analysis, scanning electron microscopy (SEM) and transmission electron microscopy (TEM). Mechanical properties were also investigated for these nanocomposites. The nanocomposites showed increasing mechanical properties and thermal stability. XRD results indicated that the materials formed nanocomposites. SEM morphology showed that increasing content of OMMT reduced the domain size of phase separated particles. TEM outcomes have confirmed the intercalated type of nanocomposite. Additionally, a solution casting process has been used to prepare these nanocomposites and characterized to compare these results with the above process.

W. H. Hoidy (✉)
Department of Chemistry, Faculty of Science, University Putra Malaysia (UPM), 43400 Serdang, Selangor, Malaysia
e-mail: Wisam92@yahoo.com

E. A. J. Al-Mulla
Department of Chemistry, College of Science, University of Kufa, AnNajaf, Iraq
e-mail: emadaalmulla@yahoo.com

K. W. Al-Janabi
Department of Chemistry, College of Education, University of Baghdad, Dis. 314, Baghdad, Iraq
e-mail: Khalid.janabi@gmail.com

Published online: 14 September 2010

Keywords Nanocomposite · Clay modification · Poly(L-lactic acid) · Poly(caprolactone) · PLLA/PCL

Introduction

Plastic accumulation attracts the attention of scientists around the world who believe that using biodegradable polymers will solve this problem and save the environment. In this area, aliphatic polyesters play a crucial role [1].

There is a series of biodegradable aliphatic polyesters now produced on a commercial level by several companies. Among them, poly(lactic acid) (PLLA) and poly(ε-caprolactone) (PCL) appear to be the most attractive because of their availability and biodegradability. Both PLLA and PCL can be obtained through the petro-chemical route and PLLA is now available from renewable resources as well. Therefore, PLLA and PCL present a great potential with respect to applications in agriculture and in everyday life as biodegradable packaging material [2]. There are many limitations of these biodegradable polymers that include poor thermal and mechanical resistance, gas barriers properties, and access to industrialized sectors [3]. These obstacles could be controlled by enhancing polymer thermal and mechanical properties through copolymerization, blending and filling techniques. In fact, the addition of nano-sized fillers would effectively confer multifunctional enabling properties to these polymers.

In the last few decades, addition of nanofillers to polymers has drawn wide attention for the potential of these fillers to influence a number of polymer properties. For example, polymer layered silicate nanocomposites, because of the nanometer size of the silicate sheets, exhibit, even at low filler content (1–5 wt%), markedly improved mechanical, thermal, barrier and flame retardance properties, in

comparison to the unfilled matrix and to the more conventional microcomposites [4, 5].

Many reports on the characterization and categories of biodegradable polymers based on nanocomposites were explored. Paul et al. reported on the preparation of PLLA/MMT nanocomposites by a melt intercalation technique using a MMT modified with bis-(2-hydroxyethyl) methyl (hydrogenated tallow alkyl) ammonium cations [6]. The preparation of PLLA based nanocomposites with three different kinds of layered silicates via solution intercalation method in *N*-dimethylacetamide was carried out by Chang et al. [7]. In a recent report, Feijoo et al. prepared biodegradable nanocomposites of amorphous poly(lactic acid) and two different types of organically modified montmorillonite obtaining nanocomposites with stacked intercalated and partially exfoliated morphologies [8]. Pantoustier et al. used the in situ intercalative polymerization method for the preparation of PCL-based nanocomposites [9]. They compared the properties of nanocomposites prepared with both pristine MMT, and amino dodecanoic acid modified PLLA/MMT and PCL nanocomposites prepared by adding two organically modified montmorillonites and one sepiolite. These were obtained by melt blending [10]. Di et al. have reported the preparation of PCL layered silicate nanocomposites using a twin-screw extruder.

Two different types of organically modified layered silicates were used for the preparation of nanocomposites and aimed at determining the dependence of clay dispersion on the processing conditions [11]. Lee et al. [12] and Paul et al. [13] studied the biodegradability of PLLA based nanocomposites in order to study their biodegradability and compost processing. They found an increased biodegradation rate as the nanocomposite samples were completely mineralized within few days. This behaviour was generally attributed to the high relative hydrophilicity of the clays, allowing an easier permeability of water into the material thus accelerating the hydrolytic degradation process. The higher the hydrophilic character of the filler, the faster the degradation of the polymer [14].

In this study, the preparation and characterization of PLLA/PCL-MMT to produce nanocomposites using different organoclays were stated. Fatty amide (FA) and octdecylamine (ODA) was employed to modify MMT. Characterization of nanocomposites was done by various apparatuses. Both melt blending and solution casting process were used to produce these nanocomposites.

Experimental

Materials

Sodium montmorillonite used in this study was obtained from Kunimine Ind. Co. Japan. Hexane was from T.J. Baker, USA. Octadecylamine was from Acros Organics, USA. Poly(L-lactic acid) was purchased from Japan. The selected grade with Paar Physica UDS 200 apparatus at 220 °C with 25 mm diameter and 0.5 mm thickness. PLA 4042D consists of 92% L-lactide and 8% D-lactide units, with polydispersity index of 2 and a density of 1.25 g cm^{-3}. Poly(caprolactone) was obtained from Solvay Caprolactone, Warrington, England. Hydrochloric acid (HCl) was from Sigma-Aldrich, Germany.

Synthesis of Fatty Amide (FA)

Palm olein (3.8 g) was dissolved in 20 mL hexane with 4 g urea by reflux at boiling point of hexane for 10 h using a thermostated round bottom flask equipped with water-cooled condenser and mechanical stirrer. After the reaction had finished (product changed to color green with copper(Π) due to its ability to form complex). The product was dissolved in hot hexane and separated from bottom layer by separating funnel. The hexane phase was cooled in an ice bath for 4 h to obtain FA and then filtered and washed by hexane three times and dried in a vacuum desiccator over phosphorous pentoxide.

Preparation of Organoclay

Organoclay was prepared by the cationic exchange process where Na ion in the montmorillonite was exchanged with alkylammonium ion in an aqueous solution. Designated amount of sodium montmorillonite (Na-MMT) was stirred vigorously in 600 mL of hot distilled water for 1 h to form a clay suspension. Subsequently, desired amount of surfactant (ODA or FA) which had been dissolved in 400 mL of hot water and desired amount of concentrated acid hydrochloride (HCl) was added into the clay suspension of (octadecylamine). After stirring vigorously for 1 h at 80 °C, the organoclay suspension was filtered and washed with distilled water until no chloride was detected with 1.0 M silver nitrate solution. It was then dried at 60 °C for 72 h. The dried organoclay was ground until the particle size was less than 100 μm before the preparation of nanocomposite. The effect of the amount of intercalation agent was studied by varying the concentration of the intercalation agent and keeping other parameters constant.

Preparation of PLLA/PCL—Clay Nanocomposites, by Solution Casting

The required amounts of PLLA and PCL were dissolved in chloroform. The PCL solution was then transferred into the PLLA solution with a dropper and continuous stirring. After all the PCL solution was transferred into the PLLA

Table 1 The amounts of PLLA, PCL and modified clay for solution casting

Sample identity	Weight of PLLA (g)	Weight of PCL (g)	Weight of organocaly (g)
8PLLA 2PCL	4.00	1.00	0.00
8PLLA 2PCL mod1	3.96	0.99	0.05
8PLLA 2PCL mod2	3.92	0.98	0.10
8PLLA 2PCL mod3	3.88	0.97	0.15
8PLLA 2PCL mod4	3.84	0.96	0.20
8PLLA 2PCL mod5	3.80	0.95	0.25
8PLLA 2PCL mod6	3.76	0.94	0.30
8PLLA 2PCL mod7	3.72	0.93	0.35
8PLLA 2PCL mod9	3.64	0.91	0.45

Table 2 The amounts of PLLA/PCL and organoclay for melt blending

Sample identity	Weight of PLLA (g)	Weight of PCL (g)	Weight of organocaly (g)
8PLLA 2PCL	32.00	8.00	0.00
8PLLA 2PCL mod1	31.68	7.92	0.40
8PLLA 2PCL mod2	31.36	7.84	0.80
8PLLA 2PCL mod3	31.04	7.76	1.20
8PLLA 2PCL mod4	30.72	7.68	1.60
8PLLA 2PCL mod5	30.40	7.60	2.00
8PLLA 2PCL mod6	30.08	7.52	2.40
8PLLA 2PCL mod7	29.76	7.44	2.80
8PLLA 2PCL mod9	29.12	7.28	3.60

solution, the resultant mixture was then stirred for 1 h. The required modified clay (FA-MMT) was then added into the dissolved PLLA/PCL in the small portion. The mixture was then refluxed for 1 h and then ultrasonically stirred using the Ultra Sonic Cathode for 5 min to make sure that the clay fully dispersed in the PLLA/PCL solution. The nanocomposite was poured into a Petri dish and left to dry. The amount of PLLA/PCL and the modified clay used are listed in Table 1.

Preparation of PLLA/PCL—Clay Nanocomposite by Melt Blending

The designed amount of PLLA/PCL ratio was prepared by an internal mixer (Haake Polydrive), using different conditions (temperature, speed and time) in order to obtain the optimum conditions which were 185 °C, 50 rpm and 12 min respectively. To prepare a sample of the composite, a specific amount of PLLA was first melted and mixed thoroughly with appropriate amount of PCL for 2 min. Various amounts of organoclays (1, 2, 3, 4, 5, 6 and 7 php) were incorporated into the blend in the third minute. The mixture was compress-moulded into sheet of 1 mm thickness under a pressure of 100 kg cm^{-1} in a standard hot press at 150 °C for 15 min and cooled for 10 min to obtain a sheet [15]. The amount of PLLA, PCL and the organoclays used are listed in Table 2.

Characterization

The FTIR spectra were recorded on Perkin Elmer FTIR 1650 spectrophotometer at ambient temperature using a KBr disk method. The disk containing 0.0010 g of the sample and 0.3000 g of fine grade KBr was scanned at 16 scans at wavenumber range of 400–4000 cm^{-1}.

Elemental analyser (LECO CHNS-932) was used for quantitative analysis of amount of intercalation agent present in the organoclay. A sample of approximately 2 mg of organocly burned at 1000 °C under oxygen gaseous flow was used for this test. The sulfamethazine was used as standard.

X-ray diffraction (XRD) study was carried out using shimadzu XRD 6000 diffractometer with Cu Kα radiation ($\lambda = 0$, 15406 nm). The diffractogram was scanned in the ranges from 2° to 10° at a scan rate of 1° min^{-1}.

TG analysis using Perkin Elmer model TGA 7 Thermogravimetric analyzer was used to measure the weight loss of the samples. The samples were heated from 30 to 800 °C with the heating rate of 10 °C min^{-1} under nitrogen atmosphere at the flow rate of 20 mL min^{-1}.

SEM images of the fractured surfaces of the nanocomposites were studied using a JEOL attached with Oxford Inca Energy 300 EDXFEL scanning electron microscope operated at 20–30 kV. The scanning electron microscope photographs were recorded at a magnification of 1000× to 3000×. SEM analysis was carried out to investigate polymer splitting, polymer pull-out, debonding, matrix cracking and polymer matrix adhesion. Samples were dehydrated for 45 min before being coated with gold particle using SEM coating unit Baltec SC030 sputter coater.

The transmission electron microscopy (TEM) images were obtained by employing a transmission electron microscope Hitachi, H7100 with an accelerating voltage of 200 kV. The samples were dispersed in chloroform and diluted to the right concentration. The suspension was then dropped on to the TEM sample grid and allowed it to dry. The very thin layer on the grid was observed on the microscope.

Results and Discussion

The amount of surfactant being intercalated into the clay galleries was calculated based on elemental analysis of the

Table 3 Amounts of C, N in Na-MMT and FA-MMT respectively

Element	Amount of element presence in clay (%)	
	Na-MMT	FA-MMT
C	0.48	38.9
N	0.16	3.1

Table 4 Amount of surfactant present in the clay layers

Organoclay	Amount of intercalatant intercalated in the modified clay	
	Calculation based on atom C (mmol g^{-1})	Calculation based on atom N (mmol g^{-1})
ODA-MMT	1.53	1.41
FA-MMT	1.99	1.93

modified clays. The amounts of atom carbon and nitrogen in the sample clay were analyzed by using elemental analyzer. Na-MMT was found to contain 0.46% carbon, and 0.15% nitrogen. The percentages of carbon and nitrogen contents in the organoclay increase after the modification. The calculation is based on either carbon atom or nitrogen atom because the increase of their content is only due to the presence of the surfactant molecule. The calculation is not based on the hydrogen content as there are possibilities of water molecules trapped between the layers of the Na-MMT. The results of this calculation are given in Table 3. The maximum amount of FA-MMT adsorbed was almost equivalent to the cation exchange capacity of the clay indicating that Na ion in clay can be easily replaced by the alkylammonium ion (Table 4).

Figure 1a shows the spectrum of PLLA. The peak at 2995 cm^{-1} corresponds to alkane stretch (C–H). The C=O peak is at 1750 cm^{-1} while peak at 1187 cm^{-1} is for C–O group. Figure 1b shows spectrum of PCL. The O–H bond is at 3443 cm^{-1}. The peaks appearing at 2943 and 2866 cm^{-1} are due to the C–H stretching. The peak at 1724 cm^{-1} is due to the C=O bonding. The C–O bending is at 1167 cm^{-1}.

Figure 1c shows the spectrum of the polymer blends (PLLA/PCL). The peak at 3358 cm^{-1} corresponds to O–H bond. The C–H stretching is at 2992 and 2945 cm^{-1}. The peak at 1747 cm^{-1} is due to the C=O bonding and at 1184 cm^{-1} corresponds to the C–O bending. These groups indicate the presence of both polymers (PLLA/PCL) in the blends. The shifting observed in the Fig. 1c with comparison to Fig. 1a and b for the C–H stretching and C=O peaks indicate the formation of PLLA/PCL blend.

The FTIR spectra of the PLLA/PCL and PLLA/PCL nanocomposites are shown in Fig. 2. The spectrum of PLLA/PCL nanocomposites show the peaks at 2995 and 2943 cm^{-1} are due to the C–H stretching. The peak for C=O bending observed at 1752 cm^{-1}. The peak for C–O bending is at 1183 cm^{-1}. The peak for Si–O stretching is at 460 cm^{-1} [16].

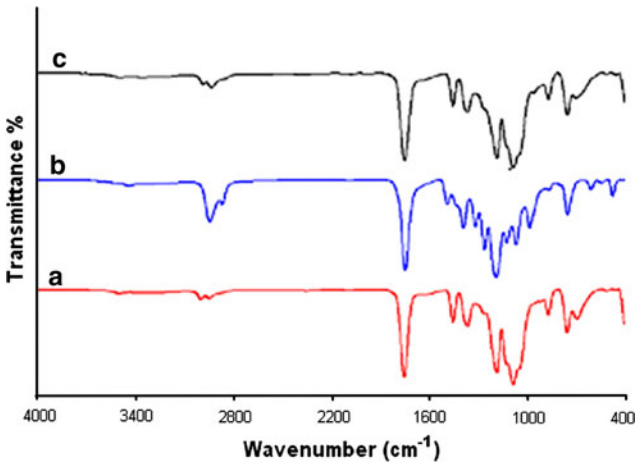

Fig. 1 FTR spectra of *a* PLLA, *b* PCL and *c* PLLA/PCL

The FTIR spectra of the FA-MMT, PLLA/PCL and PLLA/PCL nanocomposites are shown in Fig. 3. The spectrum of PLLA/PCL nanocomposites shows the peak at 3302 cm^{-1} is due to the N–H amide. The peaks at 2946 and 2891 cm^{-1} are due to the CH stretching. The peak for C=O bending absorbed at 1748 cm^{-1}. The peak for C–O bending is at 1184 cm^{-1}. The peak for Si–O stretching is at 401 cm^{-1}. The above results of FTIR were obtained when the melt blending process was used. It was found that the similar results of FTIR were obtained when solution casting process was used.

The shifting observed in the Figs. 2c and 3c with comparison to Figs. 2a, b and 3a, b, respectively for the C–H stretching and C=O peaks indicate the incorporation

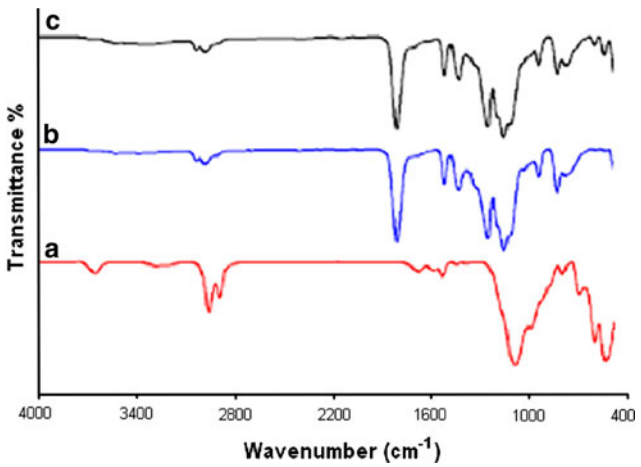

Fig. 2 FTIR spectra of *a* ODA-MMT, *b* PLLA/PCL and *c* PLLA/PCL–ODA-MMT by melt blending

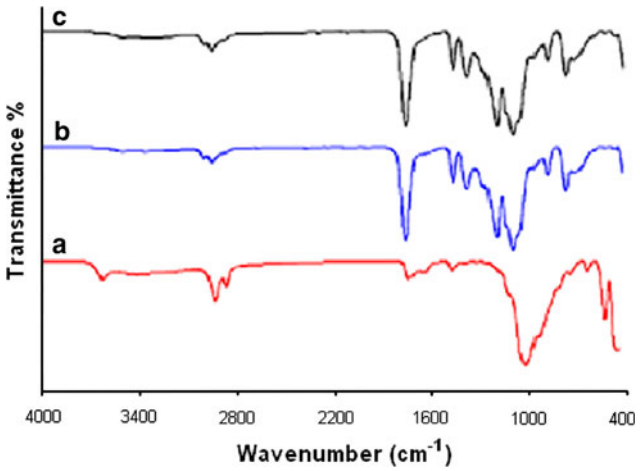

Fig. 3 FTIR spectra of *a* FA-MMT, *b* PLLA/PCL and *c* PLLA/PCL–FA-MMT by melt blending

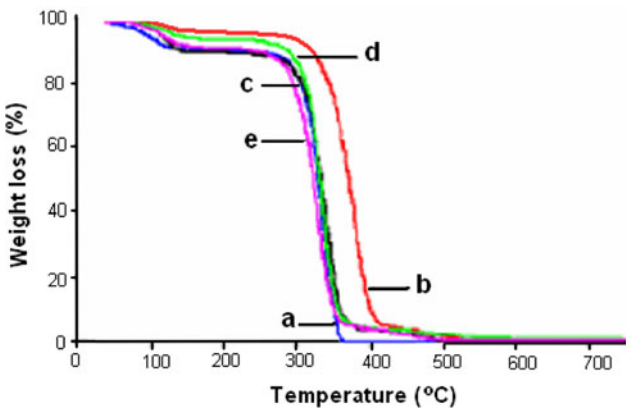

Fig. 4 TGA thermograms of *a* PLLA, *b* PCL, *c* PLLA/PCL, *d* PLLA/PCL–ODA-MMT and *e* PLLA/PCL–FA-MMT

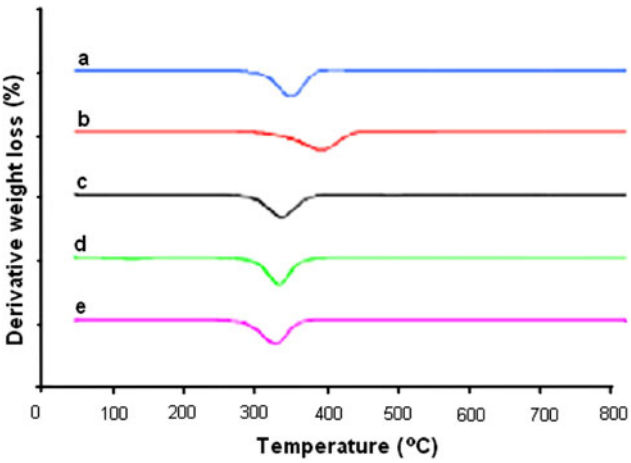

Fig. 5 DTG thermograms of *a* PLLA, *b* PCL, *c* PLLA/PCL, *d* PLLA/PCL–ODA-MMT and *e* PLLA/PCL–FA-MMT

of PLLA/PCL blend with ODA-MMT and FA-MMT modifiers, respectively.

Thermogravimetric analysis (TGA) is a quantitative measurement of mass change for a material exposed to a controlled temperature program. It also records the temperature of the weight loss region and the maximum temperature of decomposition. TGA detects single or multiple loss steps from room temperature to 1000 °C. This measurement was made to determine the thermal stability of the sample.

The sample mass loss due to the volatilizations of degraded by-product is monitored as a function of a temperature. Inorganic materials are more thermally stable and resistant compared to the organic material. Thus introduction of inorganic particles would greatly improve the thermal stability of organic materials [17].

The decomposition of PLLA starts at 187 °C. The decomposition is rapid above this temperature and completes at 384 °C. A total of 98% of weight loss was observed in the decomposition of PLLA. The DTG curve of PLLA in Fig. 5a shows a single peak at 338 °C. This decomposition corresponds to the complete dissolution of PLLA [18]. The PCL starts to decompose at around 224 °C and it completes at 444 °C. The decomposition of PCL shows a higher rate of volatile formation and higher rate of chain scission than that of PLLA which shows a single peak of DTG curve at 377 °C [19].

Thermogram of PLLA/PCL Fig. 4c shows two stages of decomposition, which corresponds to the decomposition of PLLA and PCL. The first peak of the DTG curve (Fig. 5c) occurs at 337 °C and corresponds to PLLA decomposition while the second peak occurs at 491 °C and is for PCL decomposition. After mixing PLLA with PCL, the thermal decomposition of PLLA in the blend shifts to the higher temperature region, which is 222–403 °C. The improvement of thermal stability of PLLA in the PLLA/PCL blend might be due to the presence of PCL which acts as a toughening filler of PCL as it needs more energy to degrade the blend. Chien et al. reported that the addition of PCL into PLLA improves the thermal stability of PLLA. It has been reported that the improvement of the stability can be achieved by adding a second polymer [20].

Figures 4d and 5d show the TGA and DTG thermogram of PLLA/PCL–ODA-MMT nanocomposites. The degradation temperature of the nanocomposites increase with the addition of ODA-MMT to the PLLA/PCL blend. The decomposition of PLLA/PCL–ODA-MMT nanocomposites starts at 237 °C and completes at 416 °C. The DTG curve of PLLA/PCL–ODA-MMT nanocomposites (Fig. 5d) shows a single peak at 340 °C. The temperature of the main degradation is shifted towards a higher value when OMMT is used compared to the pristine composite, it could be observed that organophilic treatment improves the

thermal stability of PLLA/PCL nanocomposites due to better interaction between PLLA/PCL matrix and clay. On the other hand, when adding FA-MMT, the thermal stability was decreased for nanocomposite. This may be due to the weak interaction between FA-MMT and the organic medium (Figs. 4e, 5e). The above results of TGA were obtained when the melt blending process was used. It was found that the similar results of FTIR were obtained for the solution casting process.

The best ratio of tensile strength and modulus properties of PLLA/PCL blending in both solution casting and melt blending was 80/20 (Fig. 6). Therefore, the ratio of 80/20 was used for further experiments.

The tensile properties of polymeric materials can be improved in different degrees if nanocomposites are formed with layered silicates. The tensile strengths of hybrid films with different OMMT contents are shown in Figs. 7 and 8. The figures show that low contents of OMMT (2 wt% and 3% for PLLA/PCL–ODA-MMT and PLLA/PCL–FAMMT, respectively) can increase the tensile strength whereas high OMMT contents in nanocomposites will cause the material to become brittle. Both PLLA/PCL–ODA-MMT and PLLA/PCL–FA-MMT nanocomposites prepared by melt blending have higher tensile strength compared with those of solution casting [21].

The XRD patterns of the PLLA/PCL–ODA-MMT and PLLA/PCL–FA-MMT nanocomposites with 1, 2, 3, 4 and 5 php of organoclay loading are given in Figs. 10, 11, 12, and 13. These results are in agreement with Yu et al. [22]. The XRD pattern of ODA-MMT and FA-MMT show peak 2θ of 3.04 and 2.89 which correspond to the basal spacing 29.68 and 31.12 Å, respectively (Fig. 9). In solution casting process the XRD of PLLA/PCL–ODA-MMT and PLLA/PCL–FA-MMT nanocomposites with 1, 2, 3, 4, and 5 php of ODA-MMT and FA-MMT show shift to lower angles between 2θ of 3.09–2.92 and 2.96–2.71 correspond

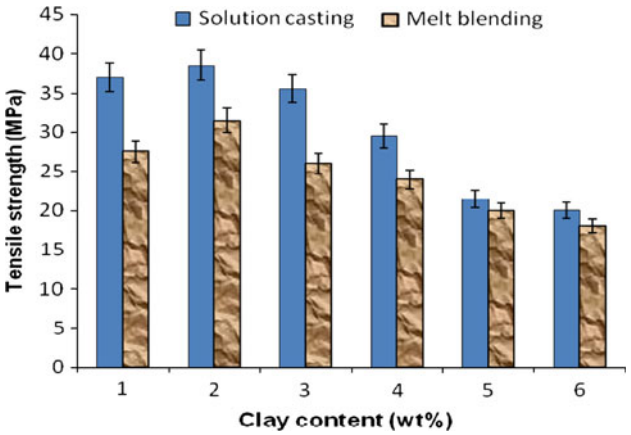

Fig. 7 Tensile strength of 80%PLLA20%PCL with various contents of ODA-MMT prepared by solution casting and melt blending

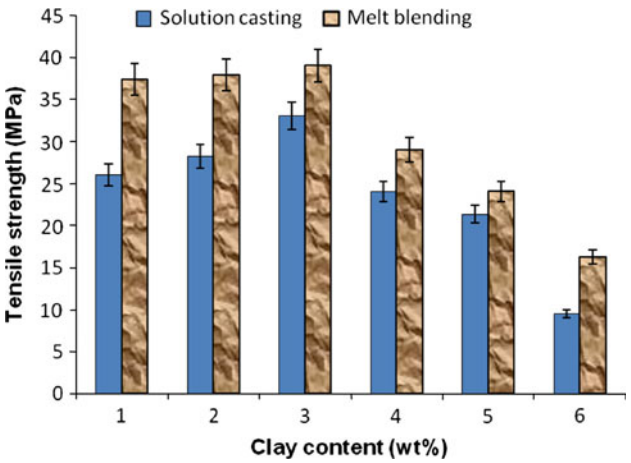

Fig. 8 Tensile strength of 80%PLLA20%PCL with various contents of FA-MMT prepared by solution casting and melt blending

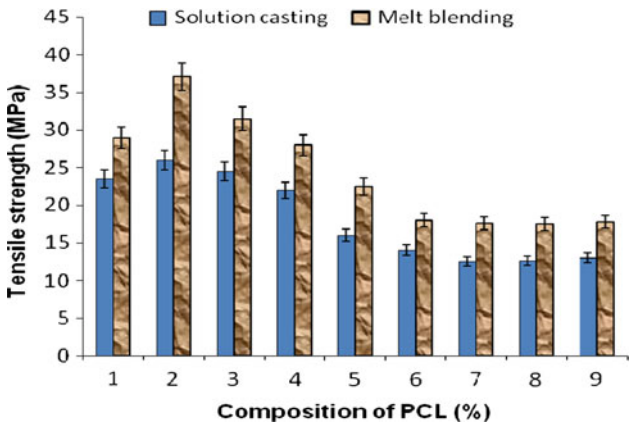

Fig. 6 Effect of adding PCL to PLLA on tensile strength by solution casting and melt blending

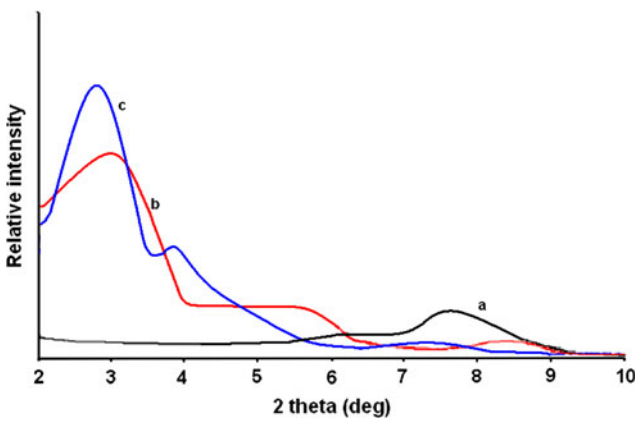

Fig. 9 The XRD patterns of *a* Na-MMT, *b* ODA-MMT and *c* FA-MMT

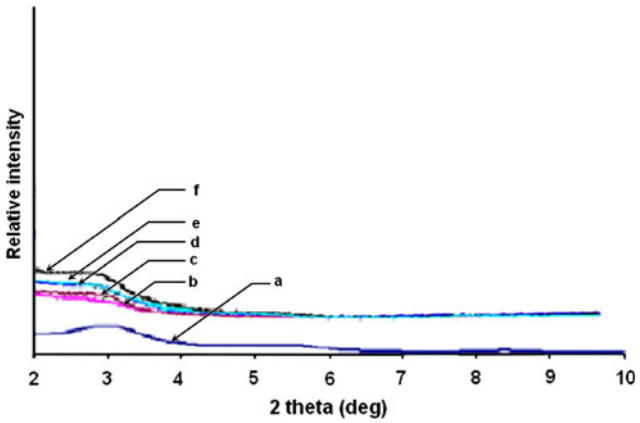

Fig. 10 XRD patterns of *a* ODA-MMT, *b* PLLA/PCL/1% ODA-MMT, *c* PLLA/PCL/2% ODA-MMT, *d* PLLA/PCL/3% ODA-MMT, *e* PLLA/PCL/4% ODA-MMT and *f* PLLA/PCL/5% ODA-MMT (by solution casting)

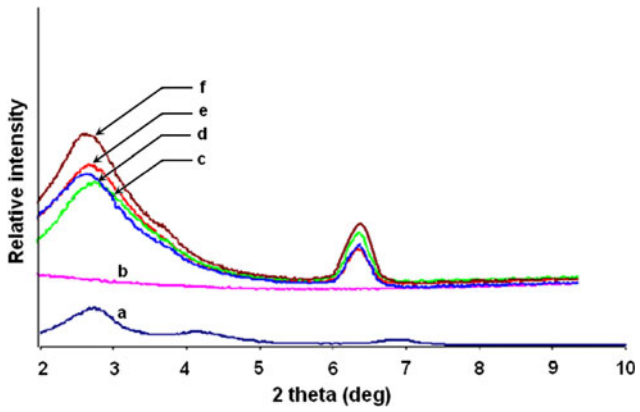

Fig. 11 XRD patterns of *a* FA-MMT *b* PLLA/PCL/1% FA-MMT, *c* PLLA/PCL/2% FA-MMT, *d* PLLA/PCL/3% FA-MMT, *e* PLLA/PCL/4% FA-MMT and *f* PLLA/PCL/5% FA-MMT (by solution casting)

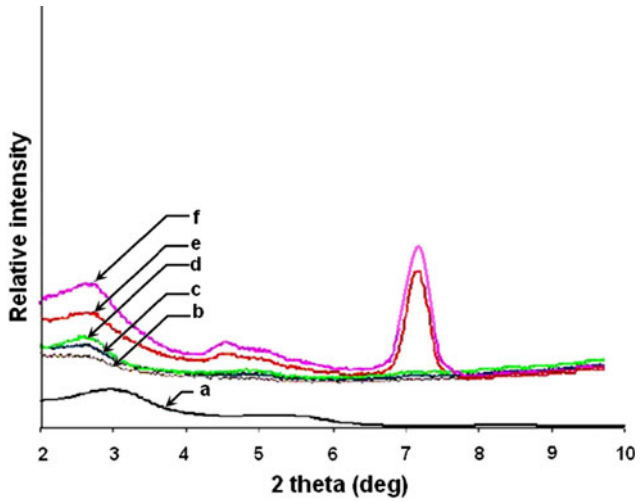

Fig. 12 XRD patterns of *a* ODA-MMT, *b* PLLA/PCL/1% ODA-MMT, *c* PLLA/PCL/3% ODA-MMT, *d* PLLA/PCL/2% ODA-MMT, *e* PLLA/PCL/4% ODA-MMT and *f* PLLA/PCL/5% ODA-MMT (by melt blending)

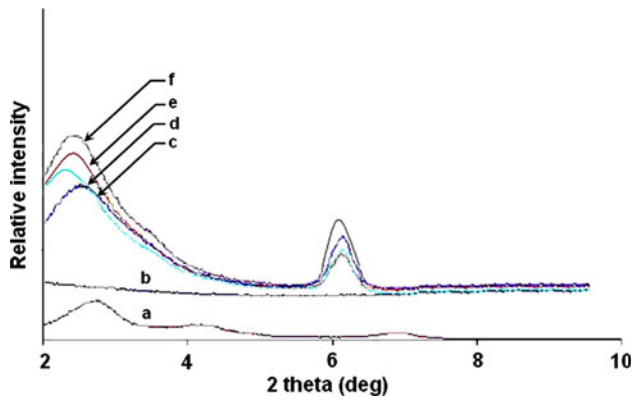

Fig. 13 XRD patterns of *a* FA-MMT, *b* PLLA/PCL/1% FA-MMT, *c* PLLA/PCL/2% FA-MMT, *d* PLLA/PCL/3% FA-MMT, *e* PLLA/PCL/4% FA-MMT and *f* PLLA/PCL/5% FA-MMT (by melt blending)

to the basal spacing between 29.91–31.07 and 30.39–33.22 Å respectively (Figs. 10, 11). While in melt blending process the XRD of PLLA/PCL–ODA-MMT and PLLA/PCL–FA-MMT nanocomposites with 1, 2, 3, 4, and 5 php of ODA-MMT and FA-MMT show shift to lower angles between 2θ of 2.80–2.61 and 2.76–2.48 correspond to the basal spacing between 32.04–34.61 and 32.5–36.18 Å respectively (Figs. 12, 13). It is found that PLLA/PCL–ODA-MMT nanocomposites with organoclay in solution casting and melt blending loading 2% give the highest basal spacing (31.04 and 34.64 Å) while the highest basal spacing of PLLA/PCL–FA-MMT nanocomposites with organoclay in solution casting and melt blending loading 3% was 33.21 and 36.18 Å, respectively. Based on the above result, the melt blending process gave higher basal spacing value compare with solution casting process. It has been noticed in (Figs. 11b, 13b) that there were no peak appeared to PLLA/PCL/1% FA-MMT since there was no effect observed for FA-MMT in the concentration 1%.

Increasing the organoclay content decreased the basal spacing because increasing the organoclay content will reduce the amount of the polymer intercalated in the galleries of the silicate layers [15]. These can be also related to the surface accessibility where the closer packing of the silicate layers is more difficult for the polymer chains to penetrate.

Figure 14 shows the SEM images of PLLA/PCL blends and PLLA/PCL with 2% ODA-MMT and PLLA/PCL with 3% FA-MMT in solution casting and melt blending in the same scale in both solution casting and melt blending

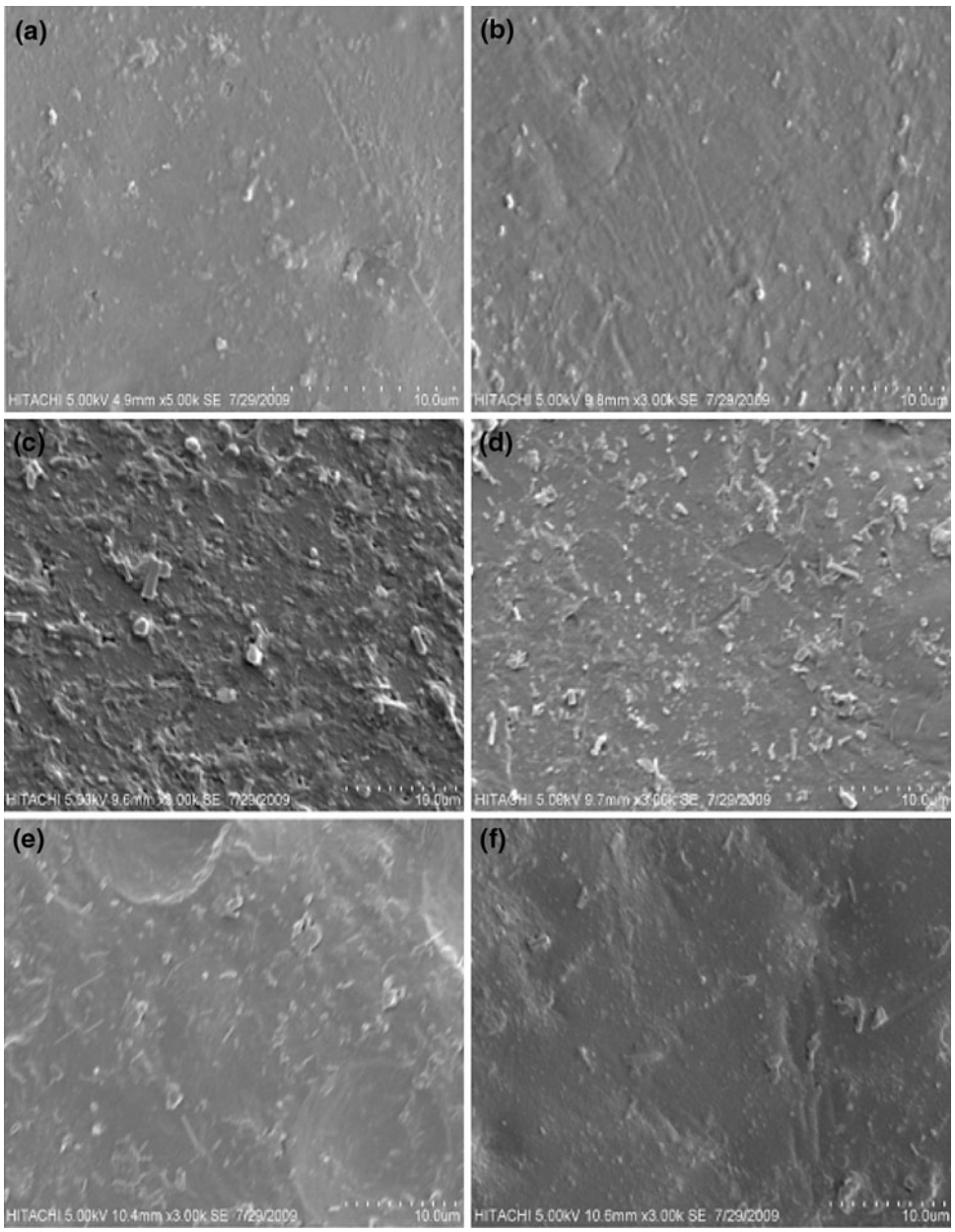

Fig. 14 SEM micrographs of (*a*) PLLA/PCL solution casting, (*b*) PLLA/PCL melt blending, (*c*) PLLA/PCL/2% ODA-MMT melt blending, (*d*) PLLA/PCL/3% FA-MMT melt blending, (*e*) PLLA/PCL/2% ODA-MMT solution casting and (*f*) PLLA/PCL/3% FA-MMT solution casting

processes, PCL was located inside of the empty voids of the PLLA continuous phase. It can be seen that the distribution of PCL in the PLLA matrix is homogenous and form single phase morphology (Fig. 14a, b).

PLLA/PCL–ODA-MMT and PLLA/PCL–FA-MMT morphology were shown in Fig. 14c and d. The incorporation of ODA-MMT and FA-MMT strongly affect the morphology, and thus also the fraction behaviour of PLLA/PCL nanocomposites which indicate the OMMT flow homogenous in the matrix and form smaller void size. This reveals that the presence of OMMT as a filler enhanced the dispersion and interfacial adhesion of polymer matrix. This observation is in agreement with the higher value of tensile strength during tensile test when OMMT is added into composites. A similar morphology was observed when the samples were prepared by solution casting process as in Fig. 14e and f.

PLLA based materials were further analyzed by TEM technique. PLLA/PCL nanocomposites by employing ODA show a high level of intercalation and exfoliation of the silicate layers (Fig. 15a), as small stacks of swollen clay layers and single dispersed layers can be observed in the TEM micrograph. The incorporation of FA in the PLLA/PCL matrix shows certain level of intercalation as well as the occurrence of micro-aggregates (Fig. 15b) of the silicate layers.

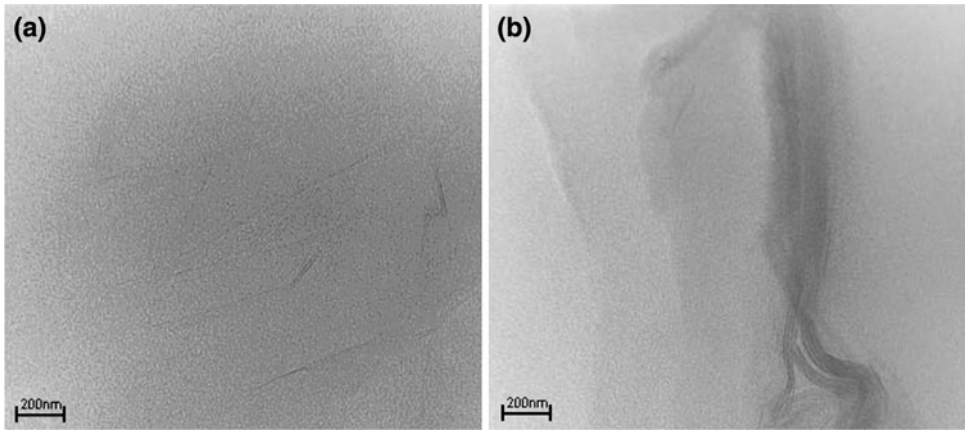

Fig. 15 TEM images of (*a*) PLLA/PCL-4% ODA and (*b*) PLLA/PCL-4% FA nanocomposites

Conclusion

PLLA/PCL–OMMT nanocomposites were prepared effectively by melt blending and solution casting. The silicate layers of the organoclay were intercalated in the polymer matrix. It is found that the highest tensile strength was observed at 80/20 (PLLA/PCL) blend. In addition to improvement of mechanical properties, the addition of OMMT to the PLLA/PCL blends significantly enhanced the thermal stability of PLLA/PCL blend when adding ODA-MMT. However, the thermal stability of PLLA/PCL blend decreased after adding FA-MMT. This may be due to the weak interaction between FA-MMT and the organic medium. The best ratios to obtain the highest basal spacing were observed when the OMMT content was 2 and 3% for ODA-MMT and FA-MMT respectively; further amount of organoclay could cause brittleness of nanocomposites. Both of PLLA/PCL–ODA-MMT and PLLA/PCL–FAM-MT nanocomposites prepared by melt blending gave higher tensile strength and basal spacing compared with those of solution casting. While it was found that the similar results of FTIR and TGA were obtained when melt blending and solution casting process was used to produce PLLA, PCL, PLLA/PCL, PLLA/PCL–ODA-MMT and PLLA/PCL–FA-MMT.

Acknowledgements The authors gratefully acknowledge Prof Dr. Mufeed Jalil Ewadh, Cultural Bureau, Embassy of the Republic of Iraq, Kuala Lumpur, Malaysia and Dr. Esam H. Hewayde, Department of Civil Engineering, College of Engineering, Al-Muthanna University for their helpful discussions and suggestions.

References

1. Franco CR et al (2004) Polym Degrad Stab 86:95–103
2. Tsuji H et al (2001) Int J Biol Macromol 29:83–89
3. Singh RP et al (2003) Carbohydr Res 338:1759–1769
4. Chow WS et al (2009) J Therm Anal Calorim 95:627–632
5. Pluta M et al (2002) J Appl Polym Sci 86:1497–1506
6. Paul MA et al (2003) Polymer 44:443–450
7. Chang JH et al (2003) J Polym Sci 41:94–99
8. Feijoo JL et al (2005) J Mater Sci 40:1785–1788
9. Pantoustier N et al (2002) Polym Eng Sci 42:1928–1933
10. Fukushima K et al (2009) Mater Sci Eng 29:1433–1441
11. Di Y et al (2003) J Polym Sci 41:670–675
12. Lee SR et al (2002) Polymer 43:2495–2500
13. Paula MA et al (2005) Polym Degrad Stab 87:535–542
14. Wang L et al (1998) Polym Degrad Stab 59:161–168
15. Vu YT et al (2001) J Appl Polym Sci 82:1391–1403
16. Tyagi B et al (2006) Spectrochim Acta 64:273–278
17. Huang X et al (2001) Macromolecules 34:3255–3260
18. Ray SS et al (2005) Prog Mater Sci 50:962–1079
19. Wu T et al (2009) Appl Clay Sci 45:105–110
20. Chen CC et al (2003) Biomaterials 24:1167–1173
21. Ray SS et al (2003) Prog Polym Sci 28:1539–1641
22. Yu Z et al (2007) Polymer 48:6439–6447